Editura AcademicPres

Available online: www.notulaebotanicae.ro

Print ISSN 0255-965X; Electronic 1842-4309

Not Bot Horti Agrobo, 2017, 45(1):28-35. DOI:10.15835/nbha45110546

Notulae Botanicae Horti Agrobotanici Cluj-Napoca

Original Article

Molecular Cloning and Characterization of an Anthocyanidin Synthase Gene in *Prunus persica* (L.) Batsch

Jiabao YE, Feng XU*, Guiyuan WANG*, Qiangwen CHEN, Tingting TAO, Qiling SONG

*College of Horticulture and Gardening, Yangtze University, Jingzhou, 434025, Hubei, China; yejiabao13@163.com; xufeng198@126.com (*corresponding authors); guiyuanwang@163.com; chenqwx@163.com; 18010872961@163.com; song70@126.com*

Abstract

To elucidate the effect of anthocyanidin synthase (ANS) gene on anthocyanin accumulation in fruit skin of *Prunus persica* (L.) Batsch cv. 'Chunmei', this study cloned and characterized an ANS gene (*PpANS*) from peach. *PpANS* (GenBank accession No. KX760117) was encoded by a 1074 bp-long open reading frame (ORF) corresponding to a polypeptide consisting of 358 amino acids with a molecular mass of 40.45 kD and an isoelectric point of 5.46. PpANS contains a conserved 2-oxoglutarate- and iron-dependent dioxygenases and non-haem dioxygenase binding regions. PpANS shared high similarities to angiosperm ANS and displayed the closest genetic relationship to *Prunus domestica*. Real-time PCR analysis indicated that *PpANS* was highly expressed in fruit skin, flesh and flowers, and peach fruit skin showed the highest transcript level of *PpANS*. Anthocyanin accumulation analysis indicated that it was highly accumulated in fruit skin and flesh of peach. Changes in the transcript level were highly correlated with anthocyanin content in the different tissues of peach. Prokaryotic expression analysis showed PpANS that protein can be expressed correctly in *E. coli*, and the size of PpANS recombinant protein was consistent with its predicted size. *In vitro* enzyme activity assay revealed that recombinant PpANS protein could catalyze the formation the cyanidin from leucocyanidin.These results indicated that *PpANS* was responsible for anthocyanin accumulation in *P. persica*.

Keywords: anthocyanin accumulation, anthocyanidin synthase, expression profile, *in vitro* enzyme activity, peach

Introduction

Peach (*Prunus persica* (L.) Batsch) is a member of family Rosaceae. In terms of land area for production, peach is the third most cultivated fruit crop in temperate regions (Dirlewanger *et al*., 2002). Moreover, a peach tree offers high economic value. Candied fruit, dried fruit, and peach sauce are products that are very popular locally (Wisniewski *et al*., 2011). Peach fruit is a healthy food that contains nutrients, namely, amino acids, proteins, fats, sugars, essential oils, minerals, amygdalin, and vitamins, which are all essential to the body (Arndt *et al*., 2001; Jha *et al*., 2012). Improvement in fruit quality has recently become an important research field in pomology. The sugar-acid ratio is thus commonly used as a quality index, acid and sugar content and composition are major determinants of peach quality (Dirlewanger *et al*., 1999). External quality is mainly determined by fruit size and skin color. In fresh peach, the most important quality is skin color, which is easily perceived by consumers. Skin coloration is possibly the index that ultimately determines whether consumers will purchase a given batch of peaches. For this reason, skin color has been significantly improved in the past decades, and peach breeders have selected primarily for intense red color at early stage of maturity (Iglesias and Echeverría, 2009).

Anthocyanins, a class of flavonoids that play a major role in coloration of fruits and most flowers (Wang *et al*., 2013). Red coloration in plants is attributed to anthocyanin accumulation usually in skin and flesh of fruits. The degree of anthocyanin accumulation largely determines the quality of grape berries (Afifi *et al*., 2003; Yoshida *et al*., 2003). Fig. 1 shows the synthesis of anthocyanins in peach and of key precursors, including 4-coumaroyl-CoA and 3×malonyl-CoA, through the flavonoid biosynthetic pathway. Anthocyanidin synthase (ANS, EC. 1114111119) catalyzes the key synthesis reaction from leucoanthocyanidin to anthocyanidin. The following reaction will occur in the process described above, that is, oxidation, dehydration, and glycosylation of various leucoanthocyanidins produce corresponding anthocyanidins. Furthermore, glycosylation, methylation, and acylation are required to convert anthocyanin into cyanidin 3-glucosides (Holton and Cornish, 1995).

Received: 27 Aug 2016. Received in revised form: 01 Mar 2017. Accepted: 09 Mar 2017. Published online: 10 Mar 2017.

The main determinant of anthocyanin accumulation in fruit is a genetic factor. The reference for environmental factors is required. Environmental factors (light, temperature, environmental stress, and loss of nutrient elements) can upregulate or downregulate the expression levels of structural and regulatory genes and correspondingly promote or inhibit synthesis and accumulation of anthocyanin, resulting in different colorations in leaves or flowers (Koes *et al*., 2005; Lepiniec *et al*., 2006). ANS is one of the key enzymes in anthocyanin biosynthesis. ANS involved in later phase of anthocyanin biosynthetic and dependent on 2-ketoglutate acid and Fe^{2+} in catalyzing conversion of colorless pigments into colored pigments in flowers (Heller *et al*., 1985; Koes *et al*., 2005). ANS is encoded by a mini-gene family in many plants. *ANS* gene have been cloned and functionally analyzed in *Theobroma cacao* (Liu *et al*., 2013), *Brassica carinata* (Yan *et al*., 2014), *Brassica juncea* (Yan *et al*., 2011), *Fructus mori* (Qi *et al*., 2014), *Punica granatum* L. (Ben-Simhon *et al*., 2015), *Malus spectabilis* (Zhang *et al*., 2015), and *Pyrus communis* L. (Yang *et al*., 2013); however, few reports on regulation of anthocyanin accumulation by *ANS* gene in peach fruit skin are available. In the present study, an ANS gene (*PpANS*) was isolated from peach fruit skin by using RT-PCR technique to determine the function of *PpANS* in peach fruit. We investigated the structure of the gene, as well as deduced the amino acid composition and the recombinant product of prokaryotic expression vector in *E. coli*. We identified the products of the incubation of recombinant PpANS protein with 3,4-cis-leucocyanidin as substrate *in vitro* through high-performance liquid chromatography (HPLC). Moreover, we determined the transcript levels of *PpANS* and accumulation pattern of anthocyanins in roots, stems, leaves, flowers, and fruit skin and flesh of peach.

Materials and Methods

Plant material

This study used the six-year-old trees of peach cv. 'Chunmei' (*P. persica*) and peach rootstock cultivars of 'Flordaguard' grown in deciduous fruit tree base in the College of Horticulture and Landscape Architecture, Yangtze University, Jingzhou, Hubei Province, China. Spatial expression profile of *PpANS* was measured from roots, stems, leaves, flowers, and fruit flesh and skin, which were immediately frozen in liquid nitrogen and stored at −80 °C until further analyses.

DNA and RNA extraction and cDNA synthesis

Different tissues of peach sample (1 g) were immediately pulverized in liquid nitrogen, filtered, and centrifuged at 12,000 × g for 10 min at 4 °C. Total RNA was extracted from the roots, stems, leaves, flowers, and fruit flesh and skin of peach by using the CTAB method as described by Xu *et al.* (2008). Genomic DNA of the peach fruit skin was extracted by using the CTAB method (Xu *et al*., 2014). Prior to the use of the total RNA and DNA, their purity, concentration, and quality were tested at OD260/280 absorbance ratio and by using spectrophotometer and 1% (w/v) agarose gel electrophoresis. First-strand cDNA was synthesized using PrimeScript™ II 1st Strand cDNA Synthesis Kit (TaKaRa, Dalian, China). The reaction mixture was 20 μl and consisted of Oligo dT Primer (1 μl), dNTP mixture (1 μl), total RNA (8 μl); 5 × Primescript buffer (4 μl), RNase inhibitor (0.5 μl), Prime Script RTase (1 μl), and RNA-free H_2O (4.5 μl). The reaction was performed at 45 °C for 20 min followed by a reaction at 75 °C for 15 min.

Cloning of full-length cDNA of PpANS

The specific primer pair ANS-FP (5′-ATGGTGAGCTCTGDTTCAGTGA-3′) and ANS-RP (5′-TCACTTGTTGAGCAAAGCTTCT-3′) were designed and synthesized (Shanghai Sangon, China) based on the transcriptome sequencing data for *P. persica*. The PCR reaction conditions were as follows: 95 °C for 3 min followed by 35 cycles at 95 °C for 30 s, 56 °C for 30 s, and 72 °C for 90 s with an extension at 72 °C for 10 min (Li *et al*., 2015). The amplified products were analyzed by 1% gel electrophoresis, purified using an AxyPrep DNA Extraction Kit, cloned into pMD19-T vector (Shanghai Sangon, China), and then sequenced (Flugge and Gao, 2005).

Bioinformatics and molecular evolution analyses

BioEdit 7.0 and MEGA 6.0 were used to construct a phylogenetic tree through the neighbor-joining method and to perform multiple alignment analysis of the amino acid sequences of ANS, respectively (Kumar *et al*., 2004; Tamura *et al*., 2007). Sequence homology searches and analysis were implemented using online bioinformatics tools (*http://www.ncbi.nlm.nih.gov*). Oligo 6 software was utilized to design the primers used in the experiment. The online tool ExPASy-ProtParam (*www.expasy*.

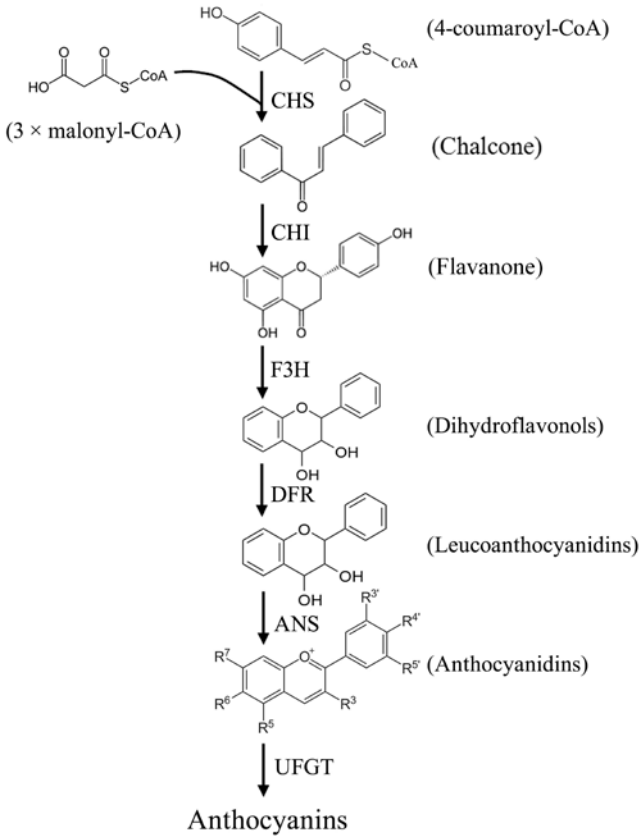

Fig. 1. Anthocyanin biosynthesis pathway in peach. CHS chalcone synthase, CHI chalcone isomerase, F3H flavanone-3-hydroxylase, DFR dihydroflavonol-4-reductase, ANS anthocyanidin synthase, UFGT glucoseflavonoid3-o-glucosyl transferase

org/tools/protparam.html) was used to deduce the molecular weight and isoelectric point (pI) of proteins (Guex *et al*., 1997; Emanuelsson *et al*., 2000).

Quantitative real-time PCR (qRT-PCR) analysis

Roots, stems, leaves, flowers, and fruit flesh and skin were sampled from peach trees. Total RNA was isolated from each sample by using the CTAB method, first-strand cDNA was synthesized using a PrimeScriptTM RT Reagent Kit (Dalian TaKaRa, China). The resulting cDNA mixtures were used to prepare the templates for qRT-PCR. The qRT-PCR product was measured using a Bio-Rad iQ5 thermal cycler with SYBR Premix Ex Taq™ II Kit (Dalian TaKaRa, China) according to the manufacturer's protocol. Expression was normalized to a gene from peach (*Pp18S*), the reference genes and primer sequences for the qRT-PCR are Pp18S-F (5′- CGGCCCATTCGA GATAACAC -3′) and Pp18S-R (5′- AGACTTATGGGAG CCGATCC -3′); ANS-RTF (5′- AACGAAAATGTGAGA GAGAG -3′) and ANS-RTR (5′- GCATTGTTTGCAA GCTTGCT -3′) were designed and synthesized by Shanghai Sangon (China). Original data were analyzed by Light Cycler software and real-time PCR data on ANS gene were calculated using the $2^{-\Delta\Delta CT}$ method as described by Livak and Schmittgen (2001).

Measurement of anthocyanin content

Anthocyanin content in the tissues of *P. persica* was assayed according to the method of Connor *et al*. (2002). One gram sample were frozen with liquid nitrogen, ground into a fine powder and extracted using 0.5 % HCl in methanol solution with shaking at 4 °C for 6 h. The extracts were centrifuged at 8,000 × g for 20 min; the supernatant was transferred into a sterile tube. Absorbance was measured at 530 nm and expressed as mg of cyanidin 3-*O*-glucoside equivalents per gram fresh weight (FW) of tissue.

PpANS expression in E. coli

The recombinant product of the prokaryotic expression vector pET32a-PpANS was constructed using the forward primer ANS-YF (5′- GCCATGGCTGATATCGATCC ATGGTGAGCTCTGATTCAGTGA -3′) and the reverse primer ANS-YR (5′- CTCGAGTGCGGCCGCAAGCT TTCACTTGTTGAGCAAAGCTTCT -3′); the underlined portion of the forward and reverse primers are the sites for enzymatic digestion, in which GGATCC was digested by *Bam*H I and AAGCTT was digested by *Hin*d III. The 1074 bp-long ORF of the amplified cDNA fragments was doubly digested by *Bam*H I and *Hin*d III, and pET32a vector (Thermo Fisher, USA) was digested with the same restriction enzymes. The target gene of *PpANS* was subsequently inserted into the pET32a vector, generating the recombinant plasmid pET32a-PpANS.

The recombinant plasmid of pET32a-PpANS was transformed into *E. coli* BL21. The transformants were incubated overnight in 20 ml of LB liquid medium containing 50 μg/ml of ampicillin at 37 °C with shaking at 200 rpm. Overnight cultures were diluted by 100-fold in LB medium, placed into 50 mg/ml ampicillin, and cultivated at 37 °C for 4 h until an A600 of 0.5-0.6 was reached. The cultures were induced with 1.0 mM isopropyl-β-D-d-thiogalactoside (IPTG) and incubated at 30 °C with shaking at 200 rpm for 4 h. The suspension was incubated in 200 μl of buffer solution at 100 °C for 5 min and centrifuged at 12, 000 × g for 15 min (Zhu *et al*., 2014). Experimental result was analyzed by sodium dodecyl sulfate polyacrylamide gel electrophoresis (SDS-PAGE) by using 12% polyacrylamide separation gel and 5% stacking gel as described by Bradford (1976). The recombinant PpANS protein was purified using View-IP™ Calmodulin Red Separopore® (Agarose) 4B-CL (BioWORD Separopore) and then used for *in vitro* enzyme assay.

Assay of PpANS activity

The enzymatic activity of recombinant PpANS was assayed using the method described by Pang *et al*. (2007) with slight modification. ANS activity was measured in a final volume of 500 μl containing 8 mmol/l sodium ascorbate, 400 mmol/l sodium chloride (NaCl), 2 mmol/l 2-oxoglutaric acid, 20 mmol/l maltose, 10 mmol/l dithiothreitol (DTT), 1 mmol/L $FeSO_4$, 1 μmol/L 3,4-cis-leucocyanidin, 40 mmol/L KPi buffer (pH 7.5), and 100 μg of purified PpANS protein. After incubation at 30 °C for 1 h, the reaction was terminated by addition of 8 μl of 18% hydrochloric acid (HCl) and 40 μl of methyl alcohol (Tanner and Kristiansen, 1993). The sample aqua was centrifuged at 12,000 × g for 5 min, and then the supernatant was passed through a 0.22 μm syringe filter according to the method described by Lockhart and Winzeler (2000). The enzymatic products were analyzed using an Agilent 1100 HPLC (Agilent Technology Co., Ltd. USA) with XDB-C18 reverse phase column (25 cm × 4.6 mm × 25 μm) (Agilent ZORBAX Eclipse, USA). The binary mobile phase used in the experiment consisted of 1% phosphoric acid and 50% methyl cyanide. Flow rate was maintained at 1 ml/min, and experimental data were measured at 530 nm. Cyanidin concentration was calculated based on a 3,4-cis-leucocyanidin standard (Sigma-Aldrich, USA). Empty pET32a vector from induced BL21 was used as control.

Results

Cloning of cDNA of PpANS

Based on the sequences of the 5′- and 3′-RACE products, full-length cDNA was deduced and amplified through PCR by using the primer pair ANS-FP and ANS-RP. The cloned full-length ORF of the *PpANS* was 1074 bp long. The G/C content in *PpANS* nucleotide sequence was 49.16% and encodes 358 amino acid with a molecular mass of 40.45 kD and a pI of 5.46. The nucleotide sequence of *PpANS* was highly similar to that of the *ANS* of other plants (Table 1). The nucleotide sequence of *PpANS* was 98%, 98%, 97%, 97%, 97%, 97%, 97%, 89%, 91%, and 91% identical to that of the ANS genes of *P. cerasifera, P. salicina* var. *cordata, P. avium, P. domestica, P. cerasus, Pyrus communis, Malus domestica, Rosa rugosa, Pyrus x bretschneideri,* and *Pyrus pyrifolia*, respectively, implying that *PpANS* is a member of the ANS gene family. Furthermore, the homology of ANS gene sequence among different species suggested that ANS was strongly conserved during molecular evolution.

Characterization of the deduced PpANS protein

Sequence comparison through BLASTP searching (http://www.ncbi.nih.gov) showed that PpANS is highly homologous to other ANS, and multi-alignment of amino acid

Table 1. Nucleotide sequence of *PpANS* similarity to the ANS genes of other plant species

Species	GenBank Accession No.	Identity (%)	E-value
Prunus cerasifera	AKV89246.1	98	0.0
Prunus salicina var. *cordata*	AEN19292.1	98	0.0
Prunus avium	AEO79983.1	97	0.0
Prunus domestica	AHZ30597.1	97	0.0
Prunus cerasus	AJO67980.1	97	0.0
Pyrus communis	AGL50919.1	92	0.0
Malus domestica	AAD26205.1	92	0.0
Rosa rugosa	AKT74337.1	89	0.0
Pyrus × *bretschneideri*	AJD00703.1	91	0.0
Pyrus pyrifolia	ADP09379.1	91	0.0

sequences (Fig. 2) showed that PpANS display high identities to *P. salicina* var. *cordata* (98%, AEN19292.1), *P. avium* (97%, AEO79983.1), *P. domestica* (97%, AHZ30597.1), *P. cerasus* (97%, AJO67980.1), *Pyrus* × *bretschneideri* (92%, AJD00703.1), *M. domestica* (92%, AAD26205.1), *R. rugosa* (89%, AKT74337.1), *Nekemias grossedentata* (85%, AGO02175.1), and *Vitis vinifera* (84%, ABV82967.1). Conserved domain searching (http://www.ncbi.nih.gov) revealed that PpANS belongs to the 2-oxoglutarate- and iron-dependent dioxygenases (2OG-Fe^{2+}-OXY) and non-haem dioxygenase (DIOX-N) superfamilies, which are characterized by the presence of the conserved domains 2OG-Fe^{2+}-OXY and DIOX-N, respectively. All of these findings indicate that PpANS is a member of the ANS family.

Analysis of the molecular evolution of PpANS

A phylogenetic tree was constructed using BioEdit 7.0 and MEGA 6.0 software to further explore the evolutionary relationships among PpANS and other proteins involved in anthocyanidin biosynthesis in plants. Phylogenetic analysis (Fig. 3) indicated that ANS genes are clearly divided into five distinct families, namely, Rosaceae, Vitaceae, Paeoniexpertae, Convolvulaceae, and Solanaceae; in addition, all of these families descended from a common progenitor. *PpANS* is closely related to *PcLDOX* (AKV89246) and clustered into a subgroup that includes *PaANS* (AEO79983), *PcANS* (ABB70119), *PbANS* (AJD00703), and *PsANS* (AMH93692), which are found in plants that also belong to Rosaceae. *PpANS* is less closely related to *IpANS* (ABW69684), *IbANS* (BAA75305), and *IhANS* (ACS71531), which are found in members of Convolvulaceae, and to *StANS* (AEJ90548), *SmANS* (ACJ02088), *IcANS* (AIY22762), *LrANS* (AHH55331), *ScANS* (AEJ90547), and *ScANS* (AEJ90547), which are found in members of Solanaceae.

Expression profile of PpANS and Anthocyanin content in different tissues

The expression pattern of *PpANS* in different tissues of *P. persica* was examined by real-time PCR. Total RNA was extracted from roots, stems, leaves, flowers, and fruit flesh and skin. As shown in Fig. 4A, *PpANS* was expressed constitutively in most plant organs but most highly expressed in fruit skin and moderately expressed in fruit flesh. By contrast, *PpANS* was weakly expressed in flowers, and the lowest expression level was

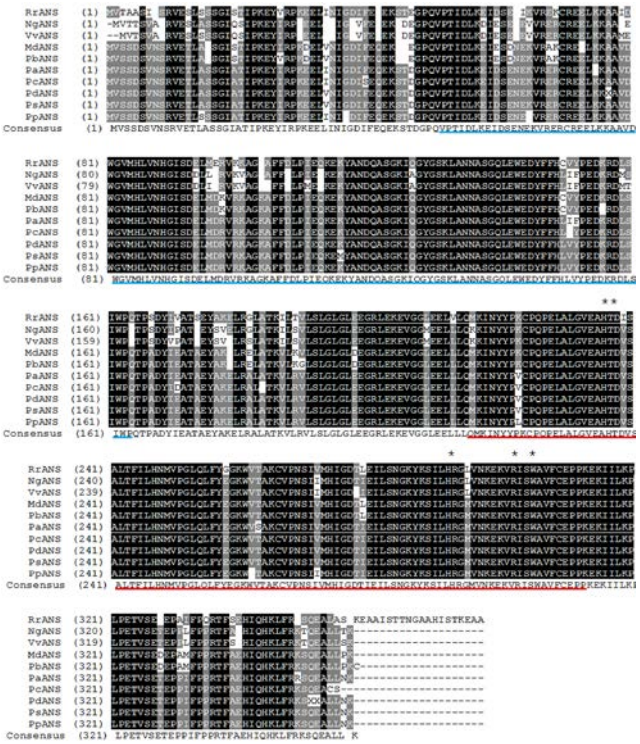

Fig. 2. Multiple alignment of PpANS with the anthocyanin synthesis in other plants. *PpANS*, *Prunus persica*; RrANS, AKT74337, *Rosa rugosa*; NgANS, AGO02175, *Nekemias grossedentata*; PbANS, AJD00703, *Pyrus* × *bretschneideri*; MdANS, AAD26205, *Malus domestica*; VvANS ABV82967, *Vitis vinifera*; PsANS, AEN19292, *Prunus salicina* var. *cordata*; PaANS, AEO79983, *Prunus avium*; PdANS, AHZ30597, *Prunus domestica*; and PcANS, AJO67980, *Prunus cerasus*. Alignment of some plant anthocyanidin synthase sequences available on GenBank. Asterisks indicate the conserved amino acid residues for ligating ferrous iron (HXD) and participating in 2-oxoglutarate binding (RXS). The 2-oxoglutarate-and iron-dependent dioxygenases conserved domain was underlined of red colour. Identical amino acids are indicated in white foreground and black background; conserve damino acids are indicated in black foreground and light gray background; block of similar amino acids are indicated in white foreground and gray background; non-similar amino acids are indicated with black foreground and white background

observed in leaves. The stems and roots of *P. persica* did not show detectable *PpANS* transcripts.

Fig. 4B shows the anthocyanin concentration of roots, stems, leaves, flowers, and fruit skin and flesh. The anthocyanins were accumulated abundantly in fruit skin, followed in the fruit flesh and flowers, and were not detected in roots. The anthocyanin content showed a good correlation with transcript level of *PpANS* in different tissues of *P. persica*. These data suggests that the expression of *PpANS* gene is one of the critical factors which determine the anthocyanin-pigmentation pattern in *P. persica*.

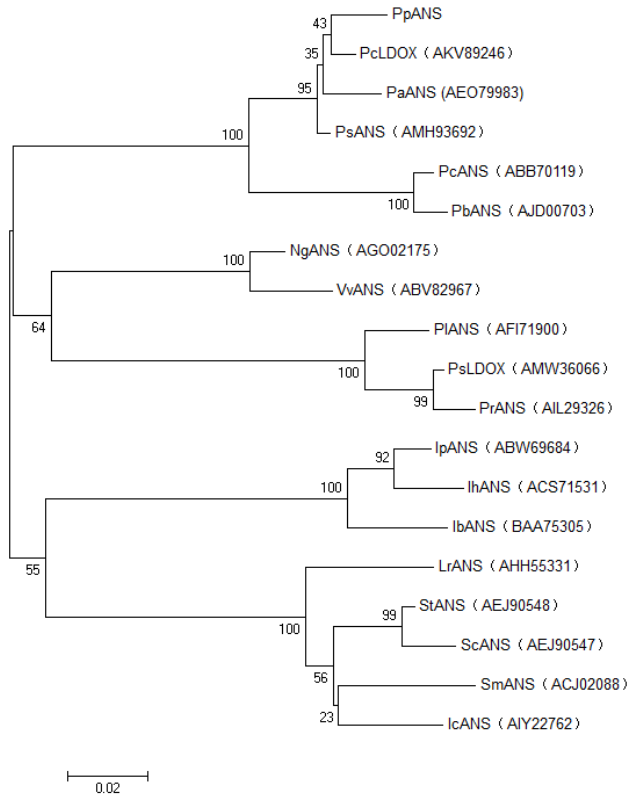

Fig. 3. Phylogenetic tree of ANS amino acid sequences from *Prunus persica* and other plant species generated by MEGA 6.0. The numbers using the neighbor-joining method and 1000 bootstrap replicates. The tree was built using the following ANS sequences: *Prunus cerasifera*, PcLDOX, AKV89246; *Prunus avium*, PaANS, AEO79983; *Pyrus communis*, PcANS, ABB70119; *Pyrus* × *bretschneideri*, PbANS, AJD00703; *Prunus salicina*, PsANS, AMH93692; *Nekemias grossedentata*, NgANS, AGO02175; *Vitis vinifera*, VvANS, ABV82967; *Paeonia suffruticosa*, PsLDOX, AMW36066; *Paeonia lactiflora*, PlANS, AFI71900; *Solanum tuberosum*, StANS, AEJ90548; *Paeonia rockii*, PrANS, AIL29326; *Ipomoea purpurea*, IpANS, ABW69684; *Solanum melongena*, SmANS, ACJ02088; *Iochroma cyaneum*, IcANS, AIY22762; *Lycium ruthenicum*, LrANS, AHH55331; *Ipomoea horsfalliae*, IhANS, ACS71531; *Solanum cardiophyllum*, ScANS, AEJ90547; and *Ipomoea batatas*, IbANS, BAA75305

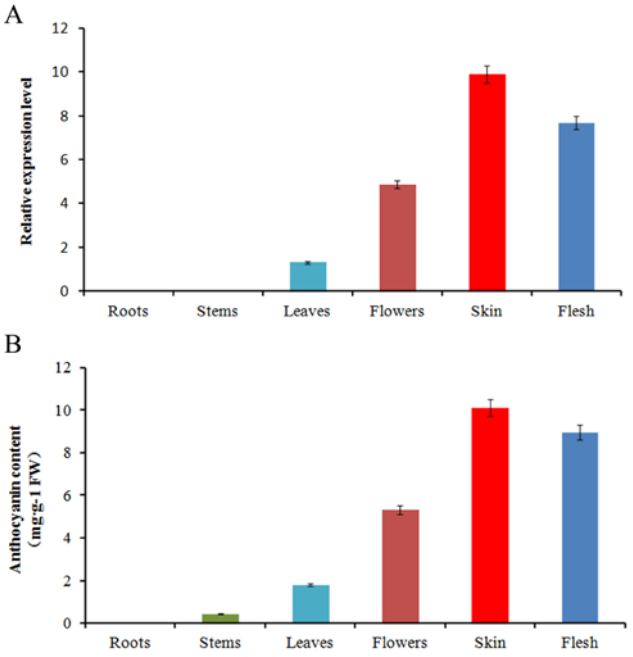

Fig. 4. Expression levels of *PpANS* gene (A) and anthocyanin content (B) in different tissues of *Prunus persica*. Analysis of expression of *PpANS* and anthocyanin content in roots, stems, leaves, flowers, skin, and flesh. Data are the mean ± SD of three replicates

Expression and assay of recombinant PpANS

To induce PpANS expression in *E. coli* BL21 cells, we cloned the coding region of PpANS into pET32a, yielding pET32a-PpANS. The constructed expression vector was checked for in-frame fusion through restriction enzyme digestion (*Hind*III and *Bam*HI) and DNA sequencing. Expression of the recombinant protein containing the 1074 bp-long ORF of PpANS was induced for 3 h with 0.5 mmol/l IPTG under stirring in the early log-phase cultures of positive clones; *E. coli* cells were subsequently recovered through centrifugation and lysed via a traditional physical-chemical process. The expected molecular mass of pET32a-PpANS protein was 40.45 kDa. SDS-PAGE profile revealed a clear protein band of 39.2-66.2 kDa (Lane 3, Fig. 5), and this band was not observed in other control, consistent with the predicted molecular mass of the translated sequences. These results suggested that recombinant PpANS proteins were expressed as inclusion bodies in *E. coli* cells.

The activity of the purified recombinant PpANS protein was assayed by using 3,4-cis-leucocyanidin as substrate in the presence of ferrous iron and 2-oxoglutaric acid. As shown in Figs. 6A and 6C, recombinant PpANS was detected by HPLC at 530 nm, and its identity confirmed as cyanidin by comparison of retention time and UV/Vis spectrum with those of authentic standards. By contrast, the empty vector control for the incubations with protein extract showed that no 3,4-cis-leucocyanidin was converted into cyanidin (Fig. 6B).

Discussion

In plants, *ANS* gene plays an important role in regular developmental processes, as well as involved in adaptation to all environmental conditions. Many *ANS* genes participating in anthocyanin biosynthesis have been cloned from plants (Reddy *et al*., 2007); however, few reports on ANS proteins in *P. persica* are available. The present study reports on one *ANS* gene (*PpANS*) isolated from the fruit skin of *P. persica*. Amino acid sequence analysis showed that PpANS protein contains a conserved structural domain consisting of 2-oxoglutarate and combination sites for iron ions and belonging to the 2OG-Fe^{2+}-OXY superfamily. This structure is composed of a conserved 2-oxoglutarate- and Fe^{2+}-dependent oxidation region, containing conserved arginine related to the combination of 2-oxoglutarate and the Fe^{2+} combination-related amino acid residues as both conserved histidine and aspartate. The structural characteristic of *ANS* gene is

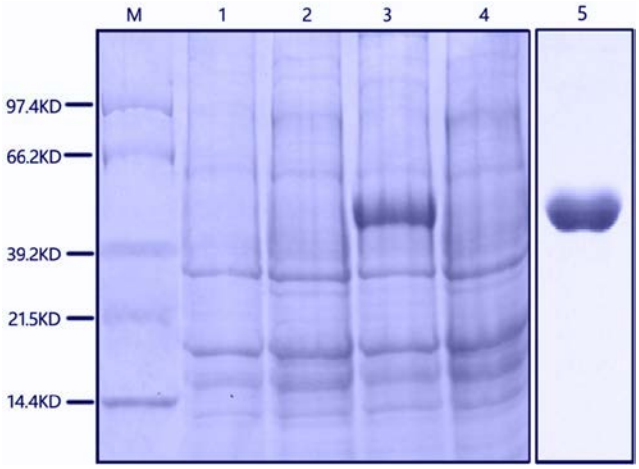

Fig. 5. SDS-PAGE electrophoresis of PpANS expressed in *E. coli* BL21. After IPTG induction, *E. coli* BL21cells containing pET32a-PpANS were grown at 30 °C for 6 h. Supernatants and pellets were examined by SDS-PAGE analysis followed by Coomassie Brilliant Blue R250 (CBB) staining. Lane M – protein molecular markers; Lane 1 – Proteins of total cells containing pET32a after 4 h induction by IPTG; Lane 2 – Proteins of total cells containing pET32a without IPTG induction; Lane 3 – Proteins of total cells containing pET32a-PpANS after 4h induction by IPTG; Lane 4 – Proteins of total cells containing pET32a-PpANS without IPTG induction. Lane 5 – Purified recombinant PpANS protein used for enzyme activity assay

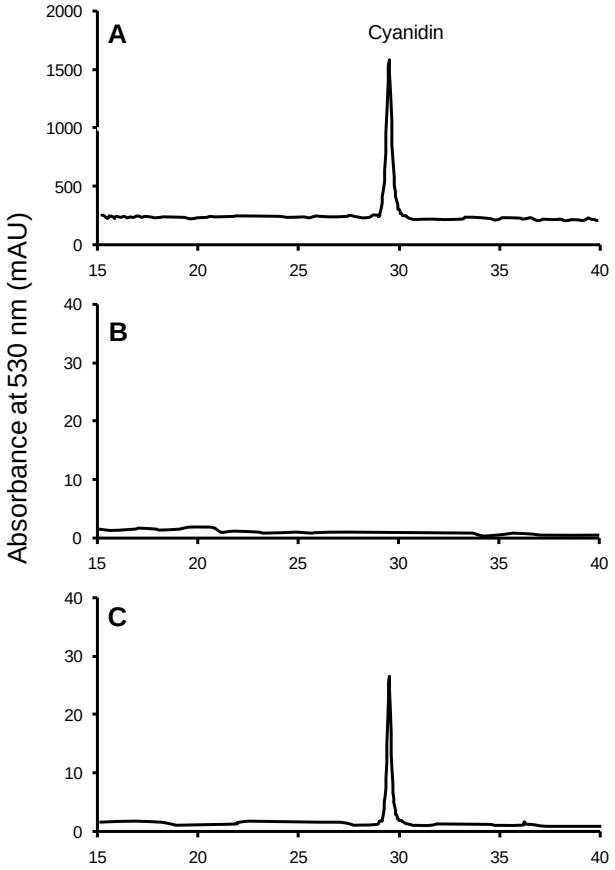

Fig. 6. HPLC analysis of the products from incubation of recombinant PpANS protein with 3, 4-cis-leucocyanidin as substrate. (A) HPLC analysis of an authentic standard of cyanidin; (B) Product form incubation of 3, 4-cis-leucocyanidin with crude protein extract from vector control; (C) Product from incubation of 3, 4-cis-leucocyanidin with purified recombinant *PpANS* by UV absorption

obviously consistent with those of the dioxygenase enzyme family, which was speculated to catalyze the formation of anthocyanidins and flavonoids in plants (Rosati *et al*., 1999). These typical features are consistent with those of *ANS* gene of other plants. The results of the sequence analysis suggest that *PpANS* facilitates the catalytic synthesis of anthocyanins. Multiple alignment of the amino acid sequence of PpANS with that of *P. cerasifera*, *P. avium*, and *P. salicina* showed that PpANS shared high identity with the homologous member of Rosaceae (Fig. 3). The evolution of PpANS resulted in distinct characteristics at the genus and species levels. Purified recombinant PpANS protein showed that PpANS can catalyze conversion of cyanidin into leucocyanidin (Fig. 6), confirming its participation in anthocyanidin biosynthetic pathway. Based on the results of the structural, functional, and sequence analyses of *PpANS*, PpANS is speculated to play the role of multifunctional dioxygenases and mediates different dioxygenase activities in anthocyanidin biosynthetic pathway in *P. persica*, consistent with previous studies in ginkgo (Xu *et al*., 2008).

The expression levels of *PpANS* in different tissues of peach trees varied (Fig. 4A). *PpANS* expression was higher in fruit skin and flesh, and flowers, and this phenomenon is possibly related to anthocyanin synthesis. Scientific research shows that these changes in transcript levels and anthocyanin accumulation at different developmental stages in the skins of peach were positively related to each other (Tsuda *et al*., 2004). *PpANS* is possibly involved in molecular regulations of coloration in peach flowers and fruits, in which large amounts of *PpANS* expression are required. This finding is consistent with that in grapes as reported by Wang *et al.* (2010). However, no *PpANS* expression was detected in stem. This result may be attributed to the use of young parts as experimental materials; these parts were still in the phase of leucoanthocyanidin synthesis, and *PpANS* remains unexpressed. These data showed that the expression levels of *PpANS*, the contents of anthocyanin were significantly consistency (Fig. 4). Our recently work showed that the dynamic changes of anthocyanin content in peach peel were similar to the changes of *ANS* gene expression levels (Ye *et al*., 2017). The changes in abundance of *PpANS* expression in different tissues of peach were synergistic with the changes in anthocyanin content, suggesting that *PpANS* is a key factor in anthocyanin synthesis in peach. Anthocyanin content changed with enzyme activity, which was controlled by abundance of *ANS* gene expression. Aharoni *et al.* (2001) inhibited *ANS* gene expression in strawberries; consequently, anthocyanin accumulation significantly decreased and then the color of corolla changed from pink to white. This study showed that the catalytic process induced by ANS in the transition from colorless anthocyanin into colored anthocyanin was one of the

most important factors in red coloration in peach. The expression of anthocyanin biosynthetic genes (*ANS*) dramatically decreased in peach leaves, resulting in a significant decrease of anthocyanin accumulation (Zhou *et al*., 2013). Nakamura *et al*. (2006) inhibited *ANS* gene expression in *Torenia fournieri* by using RNAi and found that anthocyanin content in *T. fournieri* strains was greatly reduced. *ANS* gene was mainly regulated by effect of various signals on transcription, thereby influencing the anthocyanin synthesis in plants; this finding is consistent with the results for *Litchi chinensis* as reported by Wei *et al*. (2011). To sum up, *ANS* gene exerts a regulatory function in anthocyanin synthesis.

In anthocyanin biosynthetic pathway of plant, enzymes involved in anthocyanin synthesis can catalyze conversion of colorless anthocyanin into colored anthocyanin, and the byproducts further demonstrate coupled reaction with 3-*O*-glucose transferase, and the coupling product is subsequently sent to the vacuole where colored 3-*O*-glycosylated anthocyanins form; hence, anthocyanin plays a very important role in color formation in plants (Nakajima *et al*., 2001). All the biosynthetic pathway genes, including *ANS*, showed significantly higher level of expression in red leaves than in green leaves (Zhou *et al*., 2014). ANS act as a key enzyme necessary in anthocyanin synthesis and in the metabolic pathways of anthocyanin in peach. However, little is known about the links between phenotype and genotype in coloration of flowers or fruits. In this study, the *PpANS* gene that expresses the enzyme for anthocyanin synthesis was obtained from peach fruit skin, and prokaryotic expression of its protein was performed *in vitro* to obtain purified recombinant protein showing clear target bands. This study found that *in vitro* expression of PpANS is possible. In further study, gene expression carriers for *ANS* will be established for genetic transformation and function validation to further investigate the mechanism of the role of *PpANS* in anthocyanin metabolism in peach skin and ultimately lay the foundation for molecular modification of peach fruit colors.

Conclusions

This study isolated and characterized *PpANS* from *P. persica*, and the results suggested that post-transcriptional RNA processing controls color changes in fruit skin. Although we have not yet sufficiently demonstrated the function of *PpANS*, the higher transcript levels of *PpANS* in fruit skin and flesh than in other plant tissues indicate that PpANS protein plays an active role in fruit coloration. Further characterization of the specific gene necessary to establish a color development model for *PpANS* in *P. persica*, as well as identification of specific means to improve fruit coloring by utilizing molecular breeding in *P. persica*, is a significant endeavor in future research.

Acknowledgements

This work was supported by National Natural Science Foundation of China (No. 31300574).

References

Aharoni A, De Vos C, Wein M (2001). The strawberry FaMYB1 transcription factor suppresses anthocyanin and flavonol accumulation in transgenic tobacco. Plant Journal 28(3):319-332.

Afifi M, El-Kereamy A, Legrand V, Chervin C, Monje MC, Nepveu F, Roustan JP (2003). Control of anthocyanin biosynthesis pathway gene expression by eutypine, a toxin from *Eutypa lata*, in grape cell tissue cultures. Journal of Plant Physiology 160(8):971-975.

Arndt SK, Clifford SC, Wanek W, Jones HG, Popp M (2001). Physiological and morphological adaptations of the fruit tree *Ziziphus rotundifolia* in response to progressive drought stress. Tree Physiology 21(11):705-715.

Ben-Simhon Z, Judeinstein S, Trainin T, Harel-Beja R, Bar-Yaakov I, Borochov-Neori H, Holland D (2015). A "White" anthocyanin-less pomegranate (*Punica granatum* L.) caused by an insertion in the coding region of the leucoanthocyanidin dioxygenase (LDOX; ANS) gene. PloS One 10(11):e0142777.

Bradford MM (1976). A rapid and sensitive method for the quantitation of microgram quantities of protein utilizing the principle of protein-dye binding. Analytical Biochemistry 72(1-2):248-254.

Connor AM, Luby JJ, Tong CB, Finn CE, Hancock JF (2002). Genotypic and environmental variation in antioxidant activity, total phenolic content, andanthocyanin content among blueberry cultivars. Journal of the American Society for Horticultural Science 127(1):89-97.

Dirlewanger E, Cosson P, Tavaud M, Aranzana M, Poizat C, Zanetto A, Laigret F (2002). Development of microsatellite markers in peach [*Prunus persica* (L.) Batsch] and their use in genetic diversity analysis in peach and sweet cherry (*Prunus avium* L.). Theoretical and Applied Genetics 105(1):127-138.

Dirlewanger E, Moing A, Rothan C, Svanella L, Pronier V, Guye A, Monet R (1999). Mapping QTLs controlling fruit quality in peach (*Prunus persica* (L.) Batsch). Theoretical and Applied Genetics 98(1):18-31.

Emanuelsson O, Nielsen H, Brunak S, Von Heijne G (2000). Predicting subcellular localization of proteins based on their N-terminal amino acid sequence. Journal of Molecular Biology 300(4):1005-1016.

Flugge UI, Gao W (2005). Transport of isoprenoid intermediates across chloroplast envelope membranes. Plant Biology 7:91-97.

Guex N, Peitsch MC (1997). SWISS-MODEL and the Swiss-Pdb Viewer: an environment for comparative protein modeling. Electrophoresis 18:2714-2723.

Heller W, Forkmann G, Britsch L, Grisebach H (1985). Enzymatic reduction of (+)-dihydroflavonols to flavan-3,4-cis-diols with flower extracts from *Matthiola incana* and its role in anthocyanin biosynthesis. Planta 165:284-287.

Holton TA, Cornish EC (1995). Genetics and biochemistry of anthocyanin biosynthesis. Plant Cell 7(7):1071.

Iglesias I, Echeverría G (2009). Differential effect of cultivar and harvest date on nectarine colour, quality and consumer acceptance. Scientia Horticulturae 120(1):41-50.

Jha B, Lal S, Tiwari V, Yadav SK, Agarwal PK (2012). The SbASR-1 gene cloned from an extreme halophyte *Salicornia brachiata* enhances salt tolerance in transgenic tobacco. Molecular Biotechnology 14:782-792.

Koes R, Verweij W, Quattrocchio F (2005). Flavonoids: a colorful model for the regulat ion and evolut ion of biochemical pathways. Trends Plant Science 10:236-242.

Kumar S, Tamura K, Nei M (2004). MEGA3: Integrated software for molecular evolutionary genetics analysis and sequence alignment. Brief

in Bioinformatics 5:150-163.

Lepiniec L, Debeaujon I, Routaboul JM (2006). Genetics and biochemistry of seed flavonoids. Annual Review of Plant Biology 57:405-430.

Li XG, Wang J, Yu ZY (2015). Cloning of an anthocyanidin synthase gene homolog from blackcurrant (*Ribes nigrum* L.) and its expression at different fruit stages. Genetics and Molecular Research 14(1):2726-2734.

Liu Y, Shi Z, Maximova S, Payne MJ, Guiltinan MJ (2013). Proanthocyanidin synthesis in *Theobroma cacao*: genes encoding anthocyanidin synthase, anthocyanidin reductase, and leucoanthocyanidin reductase. BMC Plant Biology 13(1):202.

Livak KJ, Schmittgen TD (2001). Analysis of relative gene expression data using real-time quantitative PCR and the $2^{-\Delta\Delta CT}$ method. Methods 25(4):402-408.

Lockhart DJ, Winzeler EA (2000). Genomics, gene expression and DNA arrays. Nature 405(6788): 827-836.

Nakajima J, Tanaka Y, Yamazaki M, Saito K (2001). Reaction mechanism from leucoanthocyanidin to anthocyanidin 3-glucoside, a key reaction for coloring in anthocyanin biosynthesis. Journal of Biological Chemistry 276:25797-25803.

Nakamura N, Fukuchi MM, Miyazaki K (2006). RNAi suppression of the anthocyanidin synthase gene in *Torenia hybrida* yields white flowers with higher frequency and better stability than antisense and sense suppression. Plant Biotechnology 23(1):13-17.

Pang Y, Peel GJ, Wright E, Wang Z, Dixon RA (2007). Early steps in proanthocyanidin biosynthesis in the model legume *Medicago truncatula*. Plant Physiology 145(3):601-615.

Qi X, Shuai Q, Chen H, Fan L, Zeng Q, He N (2014). Cloning and expression analyses of the anthocyanin biosynthetic genes in mulberry plants. Molecular Genetics and Genomics 289(5):783-793.

Reddy AM, Reddy VS, Scheffler BE, Wienand U, Reddy AR (2007). Novel trangenic rice overexpression anthocyanidin synthase accumulates a mixture of flavonoids leading to an increased antioxidant potential. Metabolic Engineering 9:95-111.

Rosati C, Cadic A, Duron M, Ingouff M, Simoneau P (1999). Molecular characterization of the anthocyanidin synthase gene in *Forsythia* × *intermedia* reveals organ-specific expression during flower development. Plant Science 149(1):73-79.

Tamura K, J Dudley, M Nei, S Kumar (2007). MEGA4: Molecular Evolutionary Genetics Analysis (MEGA) Software Version 4.0. Molecular Biology and Evolution 24:1596-1599.

Tanner GJ, Kristiansen KN (1993). Synthesis of 3, 4-cis-[3H] leucocyanidin and enzymatic reduction to catechin. Analytical Biochemistry 209(2):274-277.

Tsuda T, Yamaguchi M, Honda C, Moriguchi T (2004). Expression of anthocyanin biosynthesis genes in the skin of peach and nectarine fruit. Journal of the American Society for Horticultural Science 129(6):857-862.

Wang H, Wang W, Zhang P, Pan Q, Zhan J, Huang W (2010). Gene transcript accumulation, tissue and subcellular localization of anthocyanidin synthase (ANS) in developing grape berries. Plant Science 179(1):103-113.

Wang H, Fan W, Li H, Yang J, Huang J, Zhang P (2013). Functional characterization of dihydroflavonol-4-reductase in anthocyanin biosynthesis of purple sweet potato underlies the direct evidence of anthocyanins function against abiotic stresses. PLoS One 8(11):e78484.

Wei YZ, Hu FC, Hu GB (2011). Differential expression of anthocyanin biosynthetic genes in relation to anthocyanin accumulation in the pericarp of *Litchi chinensis* Sonn. PLoS One 6(4):e19455.

Wisniewski M, Norelli J, Bassett C, Artlip T, Macarisin D (2011). Ectopic expression of a novel peach (*Prunus persica*) CBF transcription factor in apple (*Malus* × *domestica*) results in short-day induced dormancy and increased cold hardiness. Planta 233:971-983.

Xu F, Cheng H, Cai R, Li LL, Chang J, Zhu J, Cheng SY (2008). Molecular cloning and function analysis of an anthocyanidin synthase gene from *Ginkgo biloba*, and its expression in abiotic stress responses. Molecules and Cells 26(6):536-547.

Xu F, Ning Y, Zhang W, Liao Y, Li L, Cheng H, Cheng SY (2014). An R2R3-MYB transcription factor as a negative regulator of the flavonoid biosynthesis pathway in *Ginkgo biloba*. Functional Integrative Genomics 14(1):177-189.

Yan M, Liu X, Guan C, Chen X, Liu Z (2011). Cloning and expression analysis of an anthocyanidin synthase gene homolog from *Brassica juncea*. Molecular Breeding 28(3):313-322.

Yan M, Ding S, Liu L, Yin X, Shu J (2014). Cloning and expression analysis of an anthocyanidin synthase gene homologue from *Brassica carinata*. Journal of Genetics 93(2):513-516.

Yang YN, Zhao G, Yue WQ, Zhang SL, Gu C, Wu J (2013). Molecular cloning and gene expression differences of the anthocyanin biosynthesis-related genes in the red/green skin color mutant of pear (*Pyrus communis* L.). Tree Genet Genomes 9(5):1351-1360.

Ye JB, Yang XH, Chen QW, Xu F, Wang GY (2017). Promotive effects of 5-aminolevulinic acid on fruit quality and coloration of *Prunus persica* (L.) Batsch. Scientia Horticulturae 217:266-275.

Yoshida K, Toyama-Kato Y, Kameda K, Kondo T (2003). Sepal color variation of *Hydrangea macrophylla* and vacuolar pH measured with a proton-selective microelectrode. Plant and Cell Physiology 44(3):262-268.

Zhang J, Han ZY, Tian J, Zhang X, Song TT, Yao YC (2015). The expression level of anthocyanidin synthase determines the anthocyanin content of crabapple (*Malus* sp.) petals. Acta Physiologiae Plantarum 37(6):109.

Zhou Y, Guo D, Li J, Cheng J, Zhou H, Gu C, Han YP (2013). Coordinated regulation of anthocyanin biosynthesis through photorespiration and temperature in peach (*Prunus persica* f. *atropurpurea*). Tree Genetics and Genomes 9(1):265-278.

Zhou Y, Zhou H, Lin-Wang K, Vimolmangkang S, Espley RV, Wang L, Han Y (2014). Transcriptome analysis and transient transformation suggest an ancient duplicated MYB transcription factor as a candidate gene for leaf red coloration in peach. BMC Plant Biology 14(1): 388.

Zhu L, Zhang X, Chang L, Wang A, Feng P, Han L (2014). Molecular cloning, prokaryotic expression and promoter analysis of squalene synthase gene from *Schizochytrium limacinum*. Applied Biochemistry and Microbiology 50(4):411-419.